Supporting Information

Exploration of Converting Food Waste into Value-Added Products via Insect Pretreatment-Assisted Hydrothermal Catalysis

Ouyang Li[a], Jiaming Liang[a], Yundan Chen[a], Siqi Tang[a,*] and Zhenshan Li[a,*]

[a] *College of Environmental Sciences and Engineering, State Environmental Protection Key Laboratory of All Material Fluxes in River Ecosystems, Peking University, Beijing 100871, PR China*

*Corresponding Author:

Siqi Tang, College of Environmental Sciences and Engineering, Peking University, No 5, Yi Heyuan Road, Haidian District, Beijing 100871, PR China

Phone/Fax: +86 010-62753962

E-mail: siqitang@pku.edu.cn

Zhenshan Li, College of Environmental Sciences and Engineering, Peking University, No 5, Yi Heyuan Road, Haidian District, Beijing 100871, PR China

Phone/Fax: +86 010-62753962

E-mail: lizhenshan@pku.edu.cn

Table of Contents

Text S1. Characterization methods of catalyst. 1

Text S2. Analyses of liquid samples and furfurals product. 2

Figure S1. A large version of HRTEM of Ce-HAP. 4

Figure S2. HRTEM of Ce-HAP and f(1-5) the dislocation analysis using FFT on the areas indicated by red dashed rectangles. 5

Figure S3. Mass spectra of the obtained liquids derived in the hydrothermal process with Ce-HAP (a, c, e, g, i) and (b, d, f, h, j) HAP used as catalysts under concerned conditions: (a, b) hydrothermal temperature, (c, d) holding time at target temperature, (e, f) catalyst loading, (g, h) liquid-to-solid ratio, and (i, j) initial solution pH. 6

Figure S4. The areal share of by-products under different conditions (reaction temperature, reaction duration, catalyst loading, liquid-to-solid ratio and initial solution pH) in the hydrothermal catalytic process, the bars with unshaded and shaded legends, respectively, denote the pure HAP and Ce-HAP. 7

Figure S5. Apparent appearance of the obtained liquid samples (The inserted images at the upper right corner show the stratification of the obtained liquid extracted by CH_2Cl_2): (a) hydrothermal temperature, (b) liquid-to-solid ratio, (c) initial pH, (d) reaction duration, and (e) catalyst loading. 8

Figure S6. pH of the obtained liquid samples in the hydrothermal process with Ce-HAP (shaded bars) and HAP (bare bars) used as catalysts under concerned conditions. 9

Figure S7. The areal share of by-products under the optimum condition in the HAP/Ce-HAP catalytic process and the recyclability assessment. 10

Figure S8. Ce-HAP catalyst mass change in the recyclability assessment for furfurals production. 11

Figure S9. High-resolution of Ce 3d XPS spectra of virgin Ce-HAP and cycled Ce-HAP. 12

Figure S10. The GC-MS spectrogram of the liquid obtained after catalyzing the glucose. 13

Figure S11. The carbon mass balance analysis in the hydrothermal catalysis (based on 500 mg dried BSF biomass, unit: mg). 14

Figure S12. The standard curve for furfural measurement in this work. 15

Table S1. Contents of carbohydrate monomers in the black soldier fly prepupa biomass. 16

Table S2. Contents of fatty acids in the black soldier fly prepupa biomass 17

Table S3. Contents of eighteen amino acids in the black soldier fly prepupa biomass. 19

Table S4. List of identified compounds on the obtained mass spectra of final liquids with one exemplified (reaction conditions: hydrothermal temperature of 180 ^{o}C, holding time at target

temperature of 300 min, catalyst loading of 4 wt.%, liquid-to-solid ratio (mL/g) of 300:1 and initial solution pH of 10). 21

Table S5. Experimental plan on the exploration of furfurals production from BSF feedstock in a catalytically hydrothermal process. 22

Text S1. Characterization methods of catalyst.

The X-ray diffraction (XRD) pattern of the catalyst was performed on a Bruker D8 Advance X-ray diffractor. Fourier transform infrared spectroscopy (FTIR) was carried out on a Thermo Fisher FTIR spectrometer (Nicolet iN 10, USA). Raman spectroscopy was conducted on a Renishaw inVial Reflex confocal Raman microscope operating with a 785-nm excitation laser. X-ray photoelectron spectroscopy (XPS) of the catalyst was acquired on a Thermo Fisher ESCALAB Xi+ X-ray photoelectron spectrometer. The morphology of the prepared catalyst was characterized using a ZEISS field-emission scanning electron microscope (GeminiSEM 300, Germany) and a FEI transmission electron microscopy (TEM, Talos F200X, USA). The contents of Ca, P and Ce over the catalyst was measured using a Thermo Fisher inductively coupled plasma equipped with mass spectroscopy (ICP-MS, XSeries II, USA). The thermal stability of the catalyst was assessed using a TA simultaneous thermal analyzer (Q600 SDT, USA) under N_2 flow. The profiles of acidic and basic sites of the catalyst were measured, respectively through an ammonia (NH_3)- and carbon dioxide (CO_2)- temperature programmed desorption (TPD) test performed on a Micromeritics chemisorption analyzer (AutoChem II 2920, USA).

Text S2. Analyses of liquid samples and furfurals product.

As for the obtained liquid samples, the pH was measured by an InoLab pH 720 glass meter (Weilheim, Germany). The contents of ammonium-nitrogen (NH_4-N) and nitrate-nitrogen (NO_3-N) were quantified through a Nessler's reagent-based spectrophotometry. The three-dimensional excitation-emission matrix (3D EEM) fluorescence spectra of the obtained liquids were acquired on an Agilent Cary Eclipse fluorescence spectrometer. To identify related components in the final liquid, the common organic extract dichloromethane (CH_2Cl_2) was used to prepare the analyzable sample for gas chromatography coupled with mass spectroscopy (GC-MS) analyses. 2.5 mL of liquid solution was mixed with 2.5 mL of CH_2Cl_2, then set aside for 10 min until the appearance of stratification. The organic phase lying above in the vial was transferred to a dark brownish little bottle inclusive for GC-MS analysis. The Agilent GC-MS system consisting of an Agilent 6890N GC unit and an Agilent 5973 MS cell was adopted to analyze the obtained organic phase. The equipped capillary column in the GC unit was HP-5 MS (30 m × 0.25 mm × 0.25 μm). In the settings of column temperature program, the initial temperature was set at 50 °C and held for 2 min, and then it was raised to 230 °C with a rate of 8 °C/min and retaining for 2 min. The NIST2005 database was brought into identify possible chemical compounds in accordance with observed peaks on the MS spectra obtained.

The selectivity of furfurals was calculated by the peak area of the mass spectrometry (formula S1) and external standard method was used for the quantitative analysis of

furfurals. The furfural standard with different concentration gradient was prepared and detected by GC-MS under the same conditions as the test sample and then the standard curve was obtained. According to the standard curve (Figure S12), the furfural concentrations were reached and then the furfural yields were calculated (formula S2). As stated in the text for the purpose of the design of nitrogen (N) removal efficiency, the fate of organic N present in the feedstock in the developed process should be considered due to a further separation and utilization of furfurals product. Therefore, the terminology of *nitrogen removal efficiency* was used for simplicity in data interpretation (formula S3).

$$\text{Furfural selectivity (\%)} = \frac{\text{The peak area of furfurals taking up}}{\text{The total peak area of chromatogram}} \times 100 \quad \text{(S1)}$$

$$\text{Furfural yield (\%)} = \frac{\text{Furfural concentration} \times \text{liquid volume}}{\text{The amount of the carbohydrates in the used dried BSF feedstock}} \times 100 \quad \text{(S2)}$$

$$\text{Nitrogen removal efficiency (\%)} = \frac{\frac{\text{Nitrogen concentration} \times \text{liquid volume}}{\text{The amount of dried BSF feedstock}}}{\text{The mass of N contained in the used dried BSF feedstock}} \times 100 \quad \text{(S3)}$$

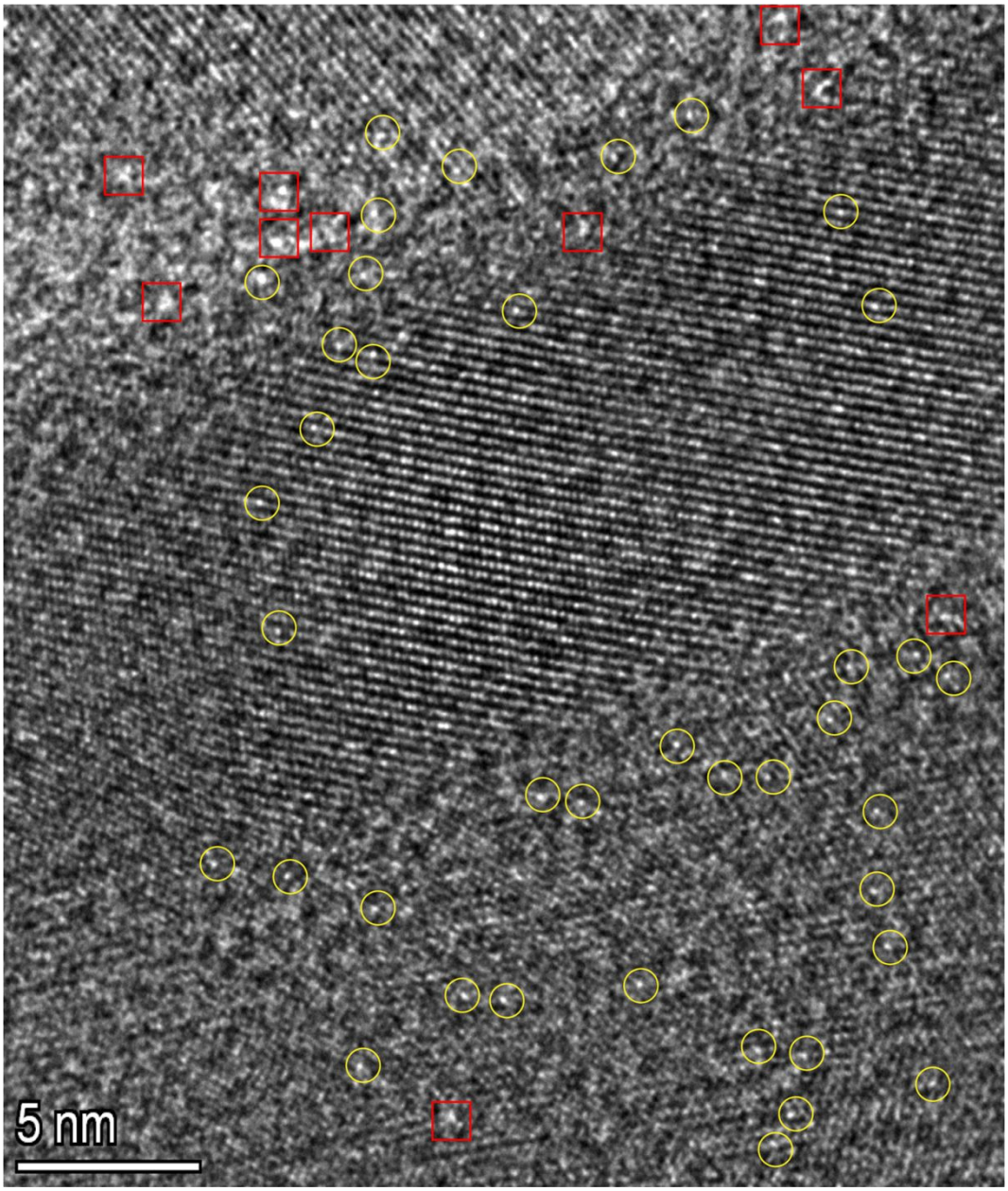

Figure S1. A large version of HRTEM of Ce-HAP.

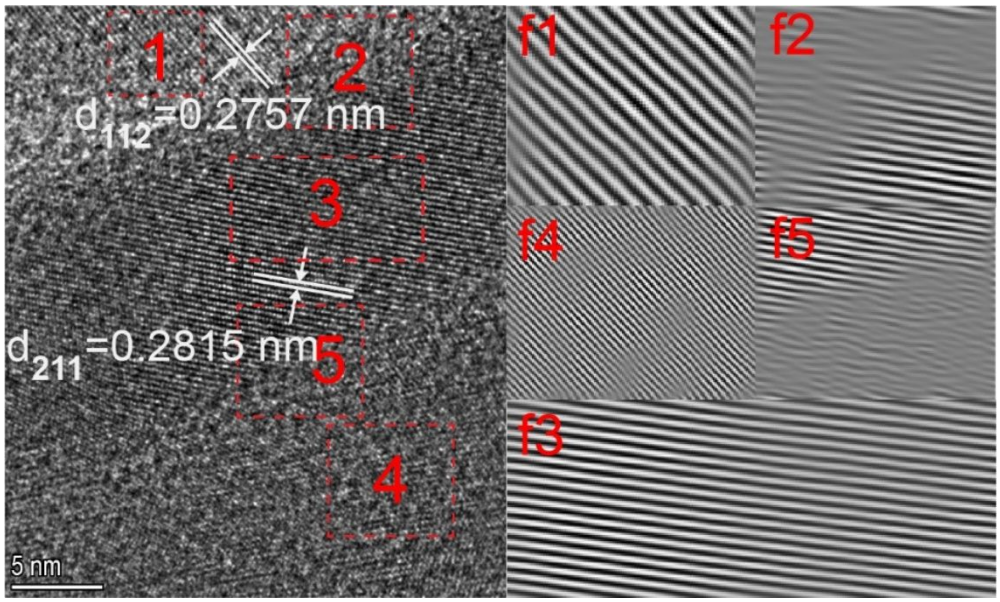

Figure S2. HRTEM of Ce-HAP and f(1-5) the dislocation analysis using FFT on the areas indicated by red dashed rectangles.

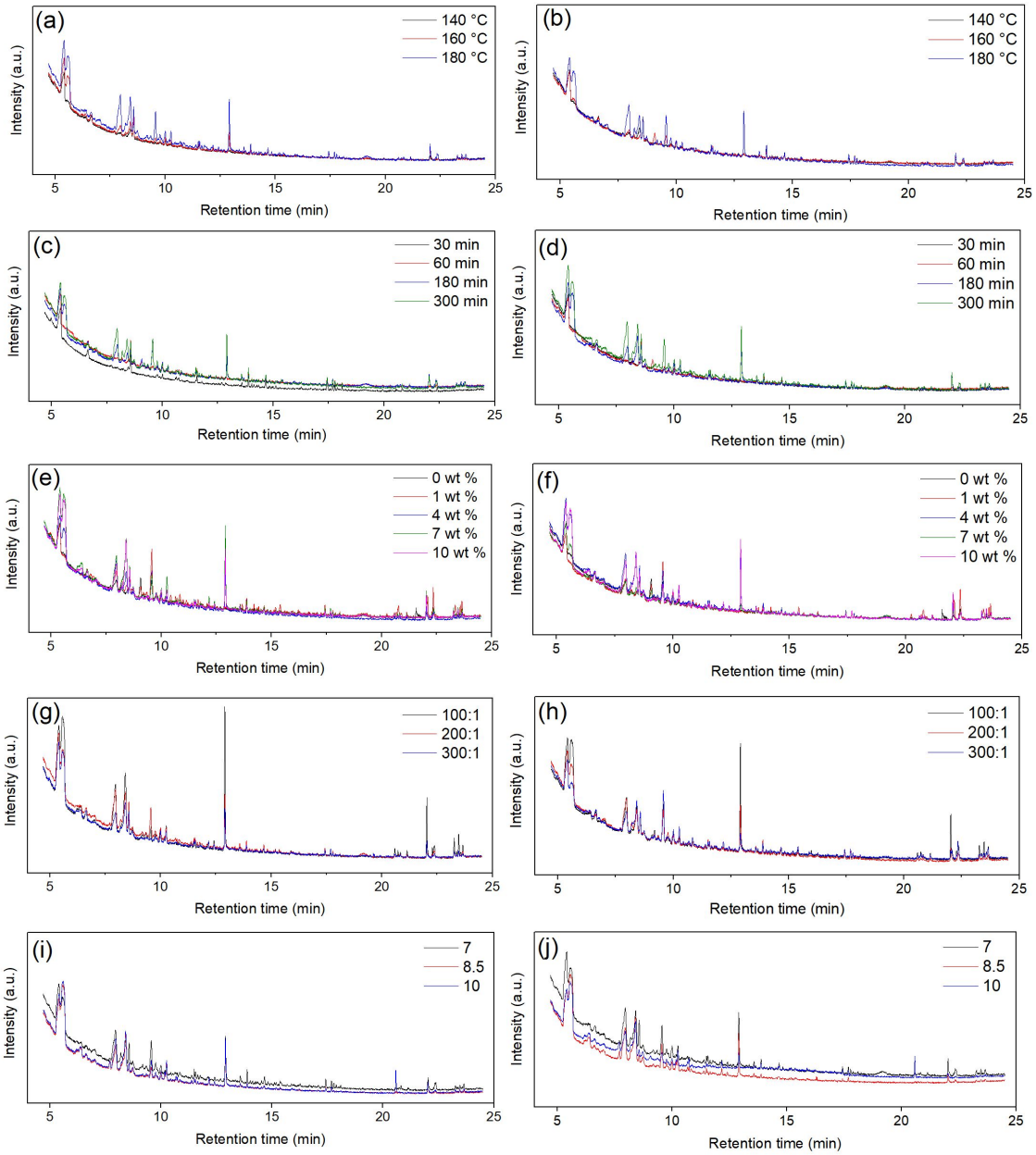

Figure S3. Mass spectra of the obtained liquids derived in the hydrothermal process with Ce-HAP (a, c, e, g, i) and (b, d, f, h, j) HAP used as catalysts under concerned conditions: (a, b) hydrothermal temperature, (c, d) holding time at target temperature, (e, f) catalyst loading, (g, h) liquid-to-solid ratio, and (i, j) initial solution pH.

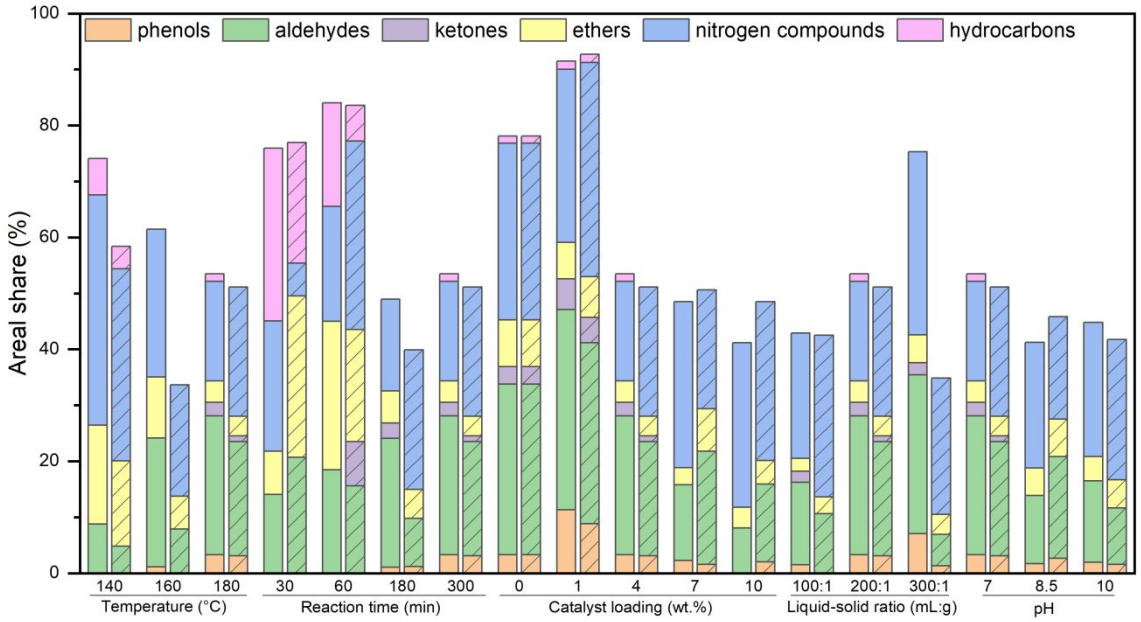

Figure S4. The areal share of by-products under different conditions (reaction temperature, reaction duration, catalyst loading, liquid-to-solid ratio and initial solution pH) in the hydrothermal catalytic process, the bars with unshaded and shaded legends, respectively, denote the pure HAP and Ce-HAP.

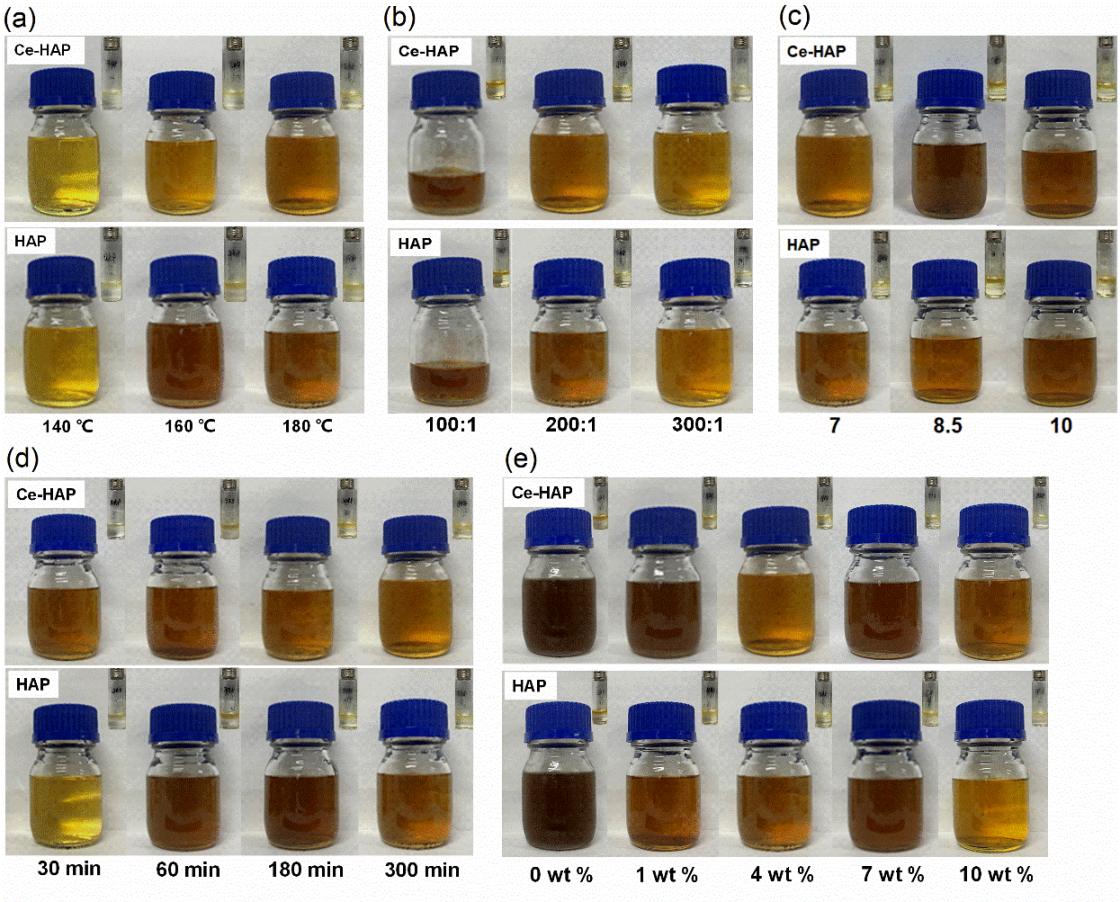

Figure S5. Apparent appearance of the obtained liquid samples (The inserted images at the upper right corner show the stratification of the obtained liquid extracted by CH_2Cl_2): (a) hydrothermal temperature, (b) liquid-to-solid ratio, (c) initial pH, (d) reaction duration, and (e) catalyst loading.

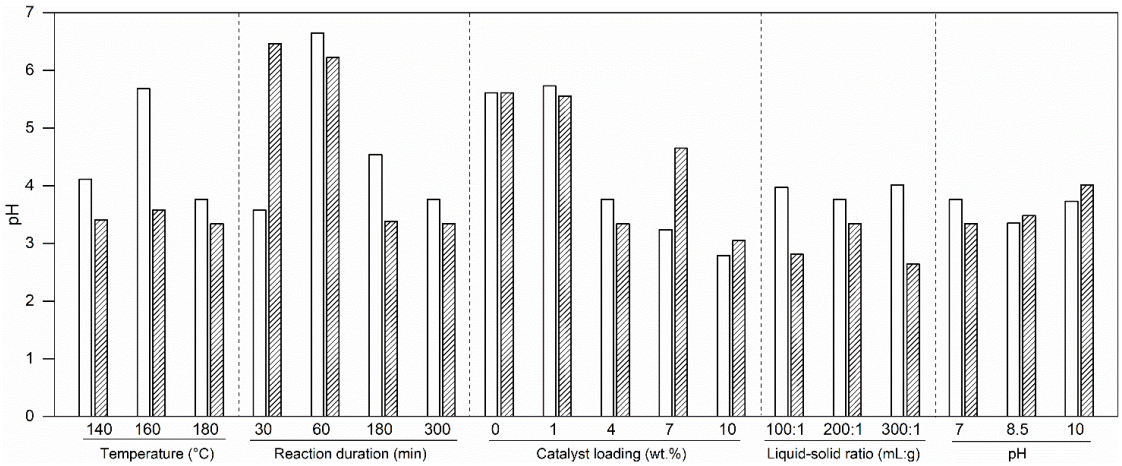

Figure S6. pH of the obtained liquid samples in the hydrothermal process with Ce-HAP (shaded bars) and HAP (bare bars) used as catalysts under concerned conditions.

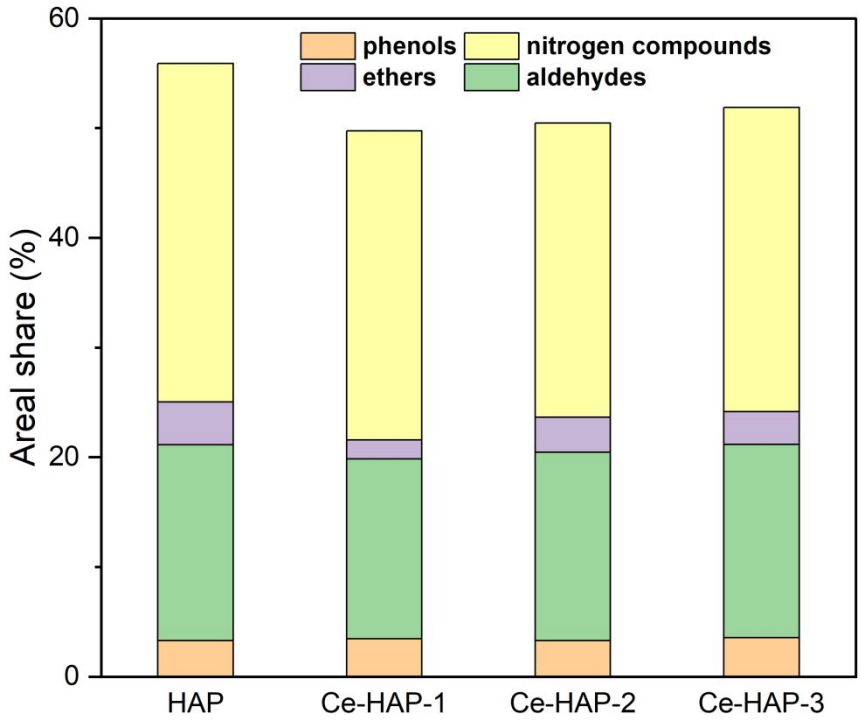

Figure S7. The areal share of by-products under the optimum condition in the HAP/Ce-HAP catalytic process and the recyclability assessment.

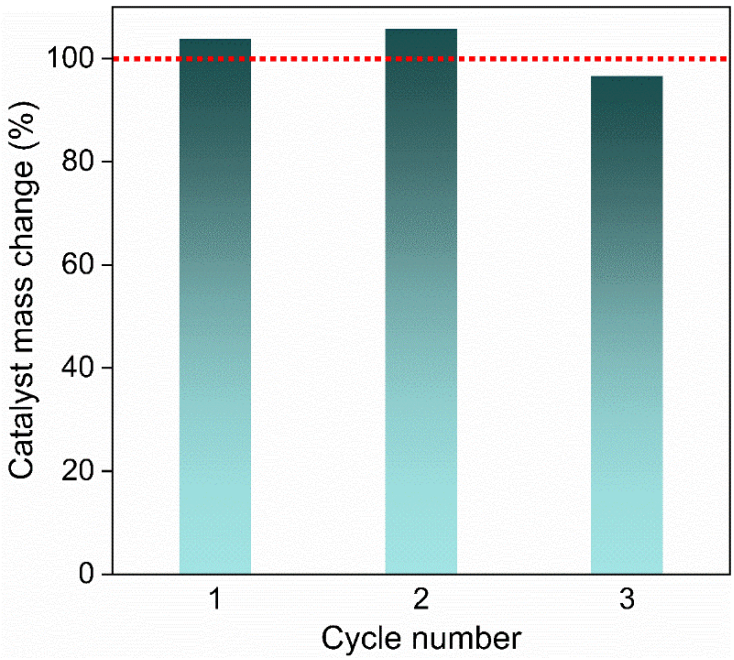

Figure S8. Ce-HAP catalyst mass change in the recyclability assessment for furfurals production.

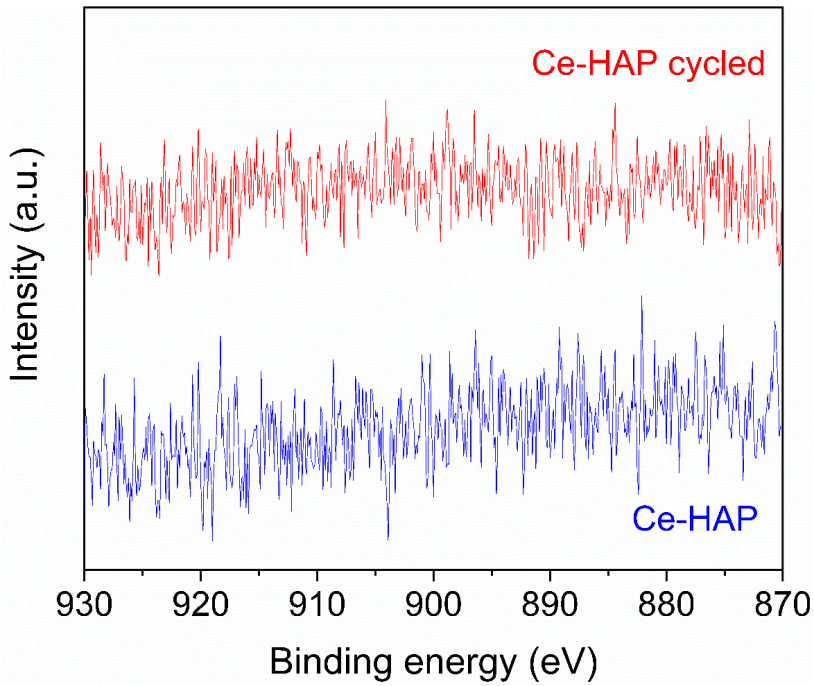

Figure S9. High-resolution of Ce 3d XPS spectra of virgin Ce-HAP and cycled Ce-HAP.

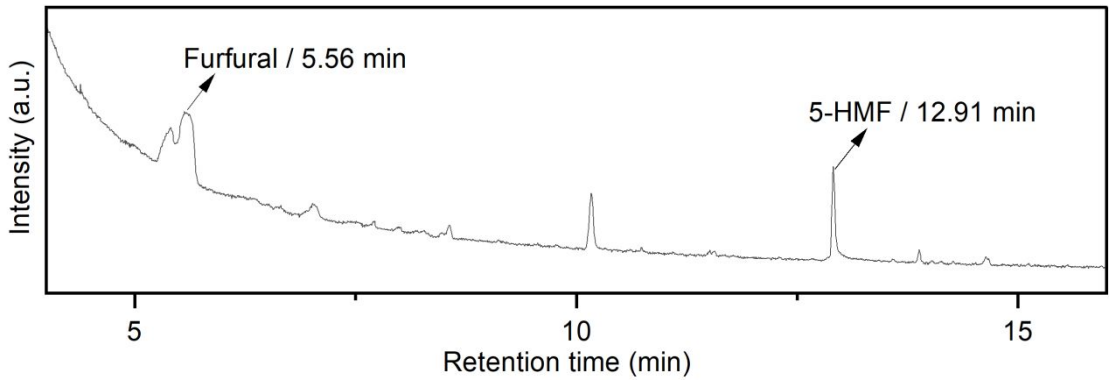

Figure S10. The GC-MS spectrogram of the liquid obtained after catalyzing the glucose.

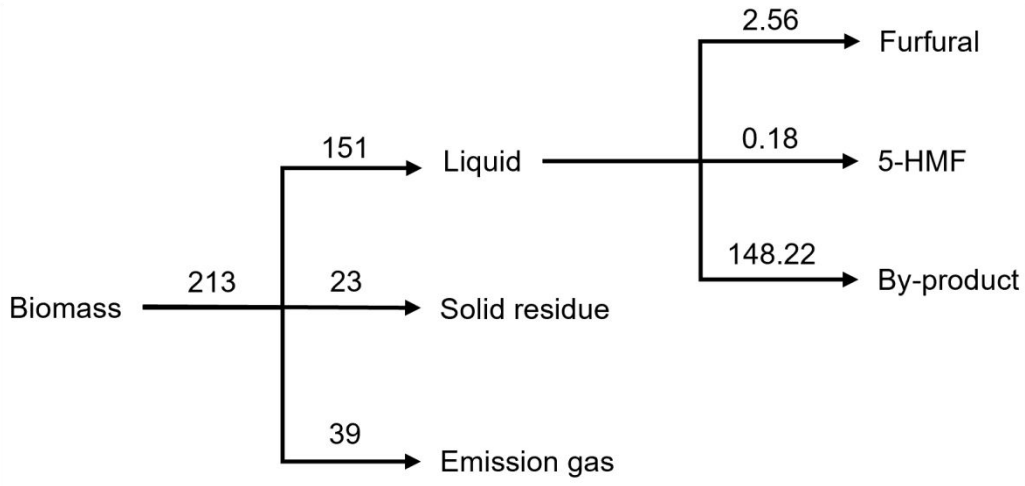

Figure S11. The carbon mass balance analysis in the hydrothermal catalysis (based on 500 mg dried BSF biomass, unit: mg).

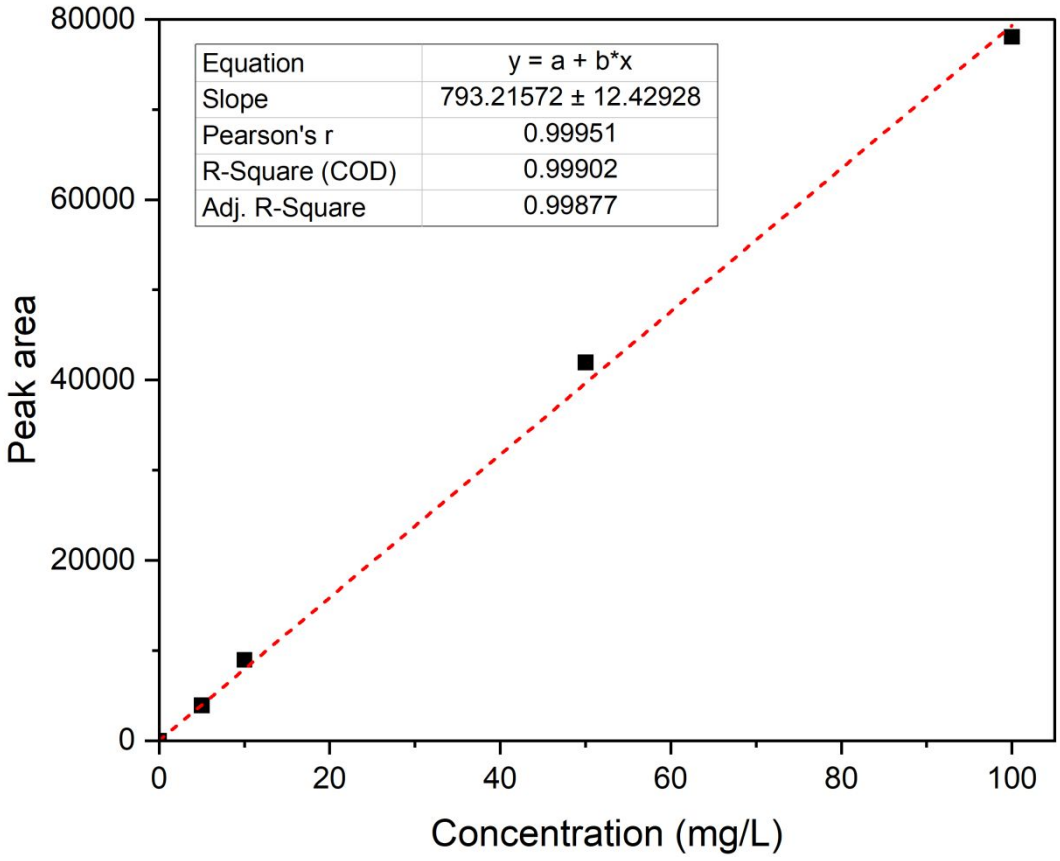

Figure S12. The standard curve for furfural measurement in this work.

Table S1. Contents of carbohydrate monomers in the black soldier fly prepupa biomass.

Carbohydrates	Contents (dry basis, wt.%)	Molecular formula	Chemical structure
Glucose	4.7	$C_6H_{12}O_6$	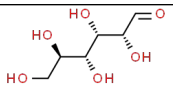
Fructose	1.2	$C_6H_{12}O_6$	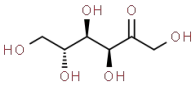
Pentose (ribose, arabinose, and xylose)	0.4	$C_5H_{10}O_5$	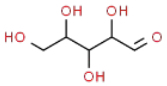
Lactose	0.5	$C_{12}H_{22}O_{11}$	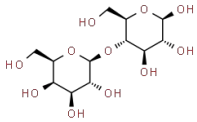
Maltose	1.8	$C_{12}H_{22}O_{11}$	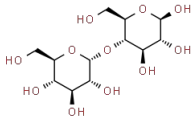

Table S2. Contents of fatty acids in the black soldier fly prepupa biomass.

Fatty acids	Contents (dry basis, wt.%)	Molecular formula	Chemical structure
Decanoic acid	0.0674	$C_{10}H_{20}O_2$	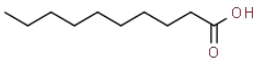
Dodecanoic acid	2.841	$C_{12}H_{24}O_2$	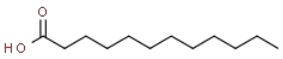
Tetradecanoic acid	0.69716	$C_{14}H_{28}O_2$	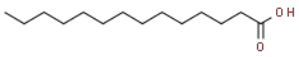
Myristic acid	0.016845	$C_{14}H_{28}O_2$	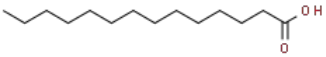
Pentadecanoic acid	0.01774	$C_{15}H_{30}O_2$	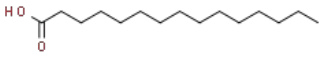
Cis-10-pentadecenoic acid	0.02043	$C_{15}H_{28}O_2$	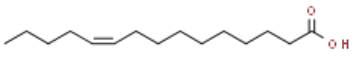
Palmitic acid	3.144	$C_{16}H_{32}O_2$	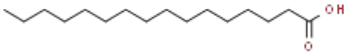
Palmitoleic acid	0.18465	$C_{16}H_{30}O_2$	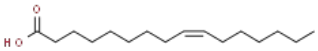
Margaric acid	0.06724	$C_{17}H_{34}O_2$	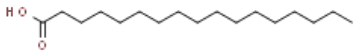
Cis-10-heptadecaenoic acid	0.02931	$C_{17}H_{32}O_2$	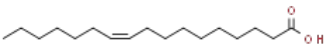
Stearic acid	0.93156	$C_{18}H_{36}O_2$	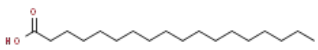
Oleic acid	4.763	$C_{18}H_{34}O_2$	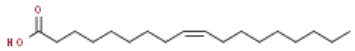
Linolelaidic acid	0.00701	$C_{18}H_{32}O_2$	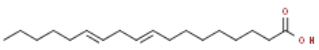
Linoleic acid	3.982	$C_{18}H_{32}O_2$	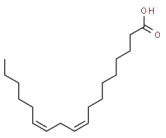
γ-Linolenic acid	0.00534	$C_{18}H_{30}O_2$	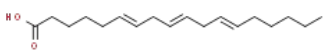
α-Linolenic acid	0.00688	$C_{18}H_{30}O_2$	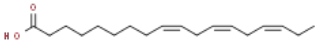

Behenic Acid	0.05458	$C_{22}H_{44}O_2$	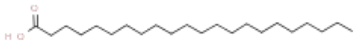
Cis-11-eicosenoic acid	0.02413	$C_{20}H_{38}O_2$	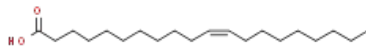
Arachidonic acid	0.01094	$C_{20}H_{32}O_2$	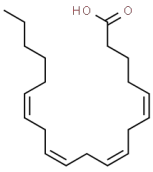
Dihomo-γ-linolenic acid	0.0065	$C_{20}H_{34}O_2$	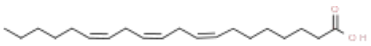
Cis-11,14,17-eicosatrienoic acid	0.115468	$C_{20}H_{34}O_2$	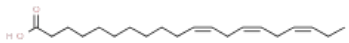
Benzoic acid	0.04377	$C_7H_6O_2$	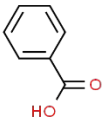
Eicosapentanoic acid	0.07463	$C_{20}H_{30}O_2$	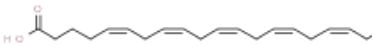
Cis-13,16-docosadienoic acid	0.00943	$C_{22}H_{40}O_2$	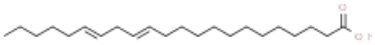
Tetradecanoic acid	0.01005	$C_{14}H_{28}O_2$	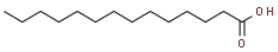
Docosahexaenoic acid	0.00701	$C_{22}H_{32}O_2$	

Table S3. Contents of eighteen amino acids in the black soldier fly prepupa biomass.

Amino acids	Contents (dry basis, wt.%)	Molecular formula	Chemical structure
Aspartic acid	3.73	$C_4H_7NO_4$	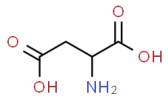
Threonine	1.99	$C_4H_9NO_3$	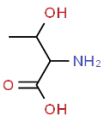
Serine	1.92	$C_3H_7NO_3$	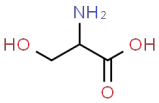
Glutamic acid	5.96	$C_5H_9NO_4$	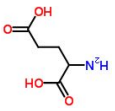
Proline	4.39	$C_5H_9NO_2$	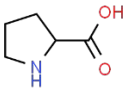
Glycine	2.99	$C_2H_5NO_2$	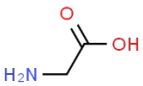
Alanine	4.27	$C_3H_7NO_2$	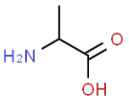
Valine	2.86	$C_5H_{11}NO_2$	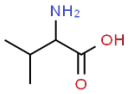
Methionine	0.62	$C_5H_{11}NO_2S$	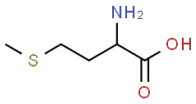
Isoleucine	2.23	$C_6H_{13}NO_2$	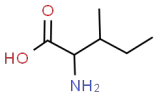
Leucine	2.95	$C_6H_{13}NO_2$	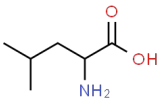
Tyrosine	2.18	$C_9H_{11}NO_3$	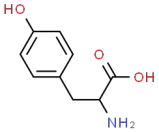
Phenylalanine	1.77	$C_9H_{11}NO_2$	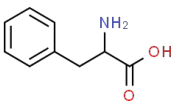

Histidine	3.96	$C_6H_9N_3O_2$	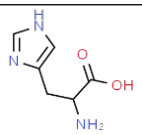
Lysine	2.98	$C_6H_{14}N_2O_2$	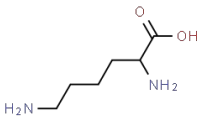
Arginine	2.5	$C_6H_{14}N_4O_2$	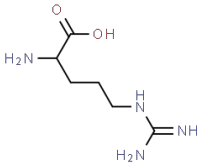
Tryptophan	0.59	$C_{11}H_{12}N_2O_2$	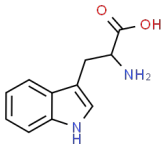
Cystine	0.48	$C_6H_{12}N_2O_4S_2$	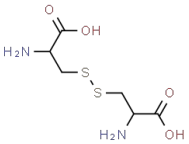

Table S4. List of identified compounds on the obtained mass spectra of final liquids with one exemplified (reaction conditions: hydrothermal temperature of 180 °C, holding time at target temperature of 300 min, catalyst loading of 4 wt.%, liquid-to-solid ratio (mL/g) of 300:1 and initial solution pH of 10).

Substance type	Substance	Retention time	Molecular formula	Chemical structure	Areal share (%)
Furans	Furfural	5.60	$C_5H_4O_2$	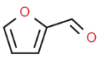	47.78
	5-Hydroxymethylfurfural	12.91	$C_7H_8O_3$	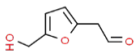	2.49
Nitrogenous compounds	Benzonitrile	8.42	C_7H_5N		21.37
	Hexanenitrile	6.38	$C_6H_{11}N$	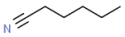	3.01
	Octanenitrile	10.26	$C_8H_{15}N$	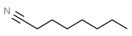	2.52
	Methyl N-hydroxybenzenecarboximidate	6.66	$C_8H_9NO_2$	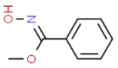	1.74
Phenols	Phenol	8.22	C_6H_6O		3.47
Aldehydes	Benzaldehyde	7.96	C_7H_6O		7.71
	Benzeneacetaldehyde	9.57	C_8H_8O		8.65
Ethers	Geranyl isovalerate	9.76	$C_{15}H_{26}O_2$	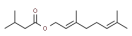	1.26

Table S5. Experimental plan on the exploration of furfurals production from BSF feedstock in a catalytically hydrothermal process.

Variable explored	Variables fixed	Values used for exploring variable
Hydrothermal temperature (℃)	Reaction duration (300 min) Catalyst loading (4 wt.%) Liquid-to-solid ratio (200 mL/g) Initial solution pH (7.0)	140, 160, 180
Reaction duration (min)	Hydrothermal temperature (180 ℃) Catalyst loading (4 wt.%) Liquid-to-solid ratio (200 mL/g) Initial solution pH (7.0)	30, 60, 180, 300
Catalyst loading (wt.%)	Hydrothermal temperature (180 ℃) Reaction duration (300 min) Liquid-to-solid ratio (200 mL/g) Initial solution pH (7.0)	0, 1, 4, 7, 10
Liquid-to-solid (mL/g)	Hydrothermal temperature (180 ℃) Reaction duration (300 min) Catalyst loading (4 wt.%) Initial solution pH (7.0)	100, 200, 300
Initial solution pH	Hydrothermal temperature (180 ℃) Reaction duration (300 min) Catalyst loading (4 wt.%) Liquid-to-solid ratio (200 mL/g)	7, 8.5, 10